



# Multimode long-wave approximation for a viscoelastic coating subject to antiplane shear

Barış Erbaş , Mikhail Itskov, Julius Kaplunov and Danila Prikazchikov

**Abstract.** A general asymptotic approach involving multimode long-wave approximations is illustrated by a 2D time-harmonic scalar problem for the dynamic antiplane shear of a viscoelastic coating. For the first time, a 1D equation of motion with the coefficients depending on frequency parameters is derived. The associated dispersion relation also seems to be a fresh development approximating its exact counterpart near the vicinities of all the cut-off frequencies. As might be expected, the developed formulation is not valid for short wavelength patterns. At the same time, as it is shown for a  $\delta$ -type loading, it proves to be robust for various scenarios dominated by long-wave response.

**Mathematics Subject Classification.** 74BXX, 74J05, 74K20, 74H10.

**Keywords.** Multimode, Long wave, Asymptotic, Coating, Viscoelastic.

## 1. Introduction

In this paper, we treat a deformable coating as a structure with one of the faces clamped and the other face subject to a prescribed loading according to the definition in [1, 2]. Coatings find numerous applications in modern technology (see e.g. [3–7] and references therein). Dynamics of elastic coatings is reasonably well studied within linear and linearized context (e.g. see [8–10]).

Our main focus is on a new type of long-wave approximations of the 2D equations of motion with a typical wavelength much greater than the thickness and not imposing any restrictions on the vibration frequency. It is well known that such structures as coatings do not exhibit low-frequency motions typical only for thin elastic plates and shells having traction free faces or loaded by prescribed stresses (e.g. see [11]). In case of clamped faces, only high-frequency, long-wave motions exist (see also [12]).

The high-frequency, long-wave vibrations relevant to the subject of the paper have been intensively investigated in various contexts (e.g. see [10, 11, 13–17], and references therein). The associated local single-mode approximations are only valid over the narrow vicinities of thickness resonances determining the cut-off frequencies.

The authors' strong desire is to establish a more general long-wave framework involving several vibration modes but not a single one as in the previous studies. This paper is aimed at deriving such multimode long-wave approximations for the scalar set-up of the antiplane shear. The simplest viscoelastic Voight model is adapted for tackling resonance phenomena. For the sake of simplicity, a typical wavelength is expressed in terms of a small viscosity coefficient.

The idea underlying the presented analysis of a basic model problem has a clear potential to be extended to many of the more sophisticated configurations in solid dynamics. The proposed approach suggests a nontraditional asymptotic scheme oriented to global long-wave approximations as an alternative to the existing local ones. Another example of a fresh insight into the asymptotic methodology utilized in the theory of thin elastic structures is concerned with the composite models for plates and shells catching

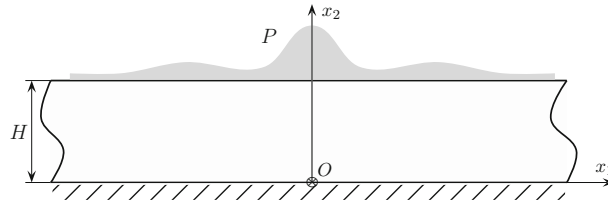


FIG. 1. A viscoelastic coating

both the canonical long-wave, low-frequency limit along with short-wave, high-frequency one related to the surface Rayleigh wave, [18, 19].

The main result of the paper is the derivation of a 1D multimode low-dimensional equation governing the antiplane shear of a viscoelastic coating. It is remarkable that the coefficients in this equation are dependent on the frequency parameter in contrast to all local single-mode formulations. The associated dispersion relation is also of multimode nature approximating the long-wave behaviour of all the vibration modes over a broad frequency range. Although the derived equation of motion, as might be expected, is not able to describe the short wavelength behaviour, it proves to be robust even for evaluating the dynamic response due to a  $\delta$ -type concentrated load. At the same time, this equation predicts a spurious fundamental (low-frequency) mode, which is not a feature of a coating due to the clamping of one of its faces.

The developed asymptotic formulation is thoroughly tested by comparison with the results obtained using the explicit exact solution of the original 2D dynamic antiplane problem. The scenario of time-harmonic free and forced vibrations is both studied.

## 2. 2D antiplane problem for a viscoelastic coating

We consider the dynamic response of a viscoelastic coating of thickness  $H$  occupying the region  $-\infty < x_1, x_3 < \infty$  and  $0 \leq x_2 \leq H$ , where  $x_n$ ,  $n = 1, 2, 3$  denote the Cartesian coordinates (see Fig. 1).

The 2D equation of antiplane motion can be written as

$$\sigma_{31,x_1} + \sigma_{32,x_2} = \rho u_{tt}, \quad (1)$$

where  $t$  is time,  $\rho$  is mass density,  $\sigma_{3i}$ ,  $i = 1, 2$  are shear stresses and  $u$  is the out of plane displacement.

The constitutive relations corresponding to the simplest viscoelastic behaviour are given by

$$\sigma_{31} = \mu u_{,1} + \gamma u_{,1t}, \quad (2)$$

$$\sigma_{32} = \mu u_{,2} + \gamma u_{,2t}, \quad (3)$$

where  $\mu$  is the shear modulus and  $\gamma$  is the viscosity coefficient. The coating is assumed to be clamped along its lower face and subject to dynamic shear loading along its upper face. The associated boundary conditions become

$$u = 0, \quad x_2 = 0, \quad (4)$$

$$\sigma_{32} = P, \quad x_2 = H, \quad (5)$$

where  $P = P(x_1, t)$  denotes a prescribed load.

Let us seek the travelling wave solution of the formulated homogeneous problem ( $P = 0$  in (5)) in the form

$$u = U(x_2) \exp\{i(kx_1 - \omega t)\} \quad (6)$$

where  $i = \sqrt{-1}$  is the complex unity,  $k$  is the wavenumber and  $\omega$  is the angular frequency.

Substituting the expression (6) in Eqs. (1)–(3), and specifying the dimensionless coordinate  $\zeta = x_2/H$  we obtain

$$\frac{d^2 U}{d\zeta^2} + \alpha^2 U = 0, \quad (7)$$

where

$$\alpha^2 = \frac{\Omega^2}{1 - i\eta\Omega} - K^2 \quad (8)$$

in which

$$K = kH, \quad \Omega = \frac{\omega H}{c_2}, \quad (9)$$

and

$$\eta = \frac{\gamma}{H\sqrt{\mu\rho}}, \quad (10)$$

where  $\eta$  is the dimensionless viscosity parameter. Below, we often assume that  $\eta \ll 1$ .

The solution to Eq. (7) satisfying the boundary condition (4) is

$$U(\zeta) = \sin \alpha \zeta. \quad (11)$$

Inserting the latter into the remaining boundary condition (5), we arrive at the dispersion relation

$$\cos \alpha = 0. \quad (12)$$

Therefore,

$$K^2 = \frac{\Omega^2}{1 - i\eta\Omega} - \Omega_*^2 \quad (13)$$

with

$$\Omega_* = \frac{(2m-1)\pi}{2}, \quad m = 1, 2, 3, \dots \quad (14)$$

standing for the cut-off frequencies of the related elastic waveguide ( $\eta = 0$ ) corresponding to its thickness shear resonances (e.g. see [11]).

In what follows, we also need the Fourier transform  $U^F$  of the time-harmonic solution of the original inhomogeneous problem (1)–(5). Omitting the factor  $\exp(-i\omega t)$ , we can readily deduce

$$u^F = \frac{P^F H}{\mu} \frac{\sin \alpha \zeta}{(1 - i\eta\Omega)\alpha \cos \alpha} \quad (15)$$

where

$$u^F = \int_{-\infty}^{\infty} u e^{iK\xi} d\xi, \quad P^F = \int_{-\infty}^{\infty} P e^{iK\xi} d\xi, \quad (16)$$

with  $\xi = x_1/H$  standing for the dimensionless longitudinal coordinate and  $K$ , now, playing the role of the Fourier transform parameter

It is worth noting that the factor  $\alpha$  in the denominator of (15) does not define the fundamental vibration mode given by  $\alpha = 0$  for which  $K = 0$  at  $\Omega = 0$  in absence of viscosity, i.e.  $\eta = 0$ . Indeed, the boundary condition (4) corresponding to a clamped lower face prohibits any low-frequency wave propagation.

Obviously, the dispersion relation (13) and the first Fourier transform in (16) take the simple explicit forms. Further insight into the asymptotic behaviour of the boundary value problem (1)–(5) underlining the aforementioned relations, (13) and (16), may be deemed unnecessary. However, such 2D formulation seems to be optimal for developing a new type of 1D asymptotic set-up corresponding to long-wave multimode approximation. In terms of the dimensionless parameters  $K$  and  $\Omega$ , this means that the wavelength of interest are much longer than the thickness of the coating ( $K \ll 1$ ), whereas there is no restriction on the vibration frequency, i.e. all modes defined by (14) are taken into consideration. To the best of authors' knowledge, previous considerations of the systems, exhibiting high-frequency

cut-offs ( $\Omega_* \sim 1$ ), as those given by (14) in the current paper, dealt only with *single-mode*, long-wave approximations in the narrow cut-off vicinities, [11]. The latter were usually referred to as high-frequency, long-wave approximations (see also [13, 14, 16, 17, 20]). In addition, we remark that the traditional theories for thin plates and shells (e.g. see [21, 22]) may be treated as low-frequency, long-wave approximations valid at small frequencies. The long-wave, low-frequency approximations are only a feature of structures with traction free faces but not typical for coatings (see the references above).

### 3. Multimode asymptotic procedure

In this section, we reduce the original 2D problem (1)–(5) to a 1D equation along the upper face of the coating  $x_2 = H$ . For the sake of simplicity, we assume that a typical wavelength is related to a small dimensionless viscosity coefficient  $\eta$  as

$$L = \frac{H}{\sqrt{\eta}}. \quad (17)$$

Thus, the ratio  $H/L = \sqrt{\eta}$  will also be small. Also, we restrict ourselves to time-harmonic motions assuming without loss of generality that the vibration frequency is order of unity ( $\Omega \sim 1$ ). Under this assumption, we are in position to treat several vibration modes (14) in contrast to previous considerations (e.g. see [10, 11, 15, 20]), oriented to narrow vicinities of chosen single cut-off frequencies  $\Omega_*$  (see (14)).

Let us scale the original coordinates as

$$x_1 = L\xi, \quad x_2 = H\zeta \quad (18)$$

nondimensionalising the displacement and stress components, as well as the external force as

$$u = Hu^*, \quad \sigma_{31} = \sqrt{\eta}\mu\sigma_{31}^*, \quad \sigma_{32} = \mu\sigma_{32}^*, \quad (19)$$

and

$$P = \mu P^*, \quad (20)$$

where the starred quantities appearing in the formula above are assumed to have the same asymptotic order. Substituting relations (18) and (19) in the equation of motion (1) and the constitutive relations (2) and (3), they, respectively, become

$$\eta\sigma_{31,\xi}^* + \sigma_{32,\zeta}^* + \Omega^2 u^* = 0 \quad (21)$$

and

$$\sigma_{31}^* = (1 - i\eta\Omega)u_{,\xi}^* \quad (22)$$

$$\sigma_{32}^* = (1 - i\eta\Omega)u_{,\zeta}^* \quad (23)$$

The boundary conditions (4) and (5) expressed through the starred quantities are written as

$$u^* = 0, \quad \zeta = 0, \quad (24)$$

$$\sigma_{32}^* = P^*, \quad \zeta = 1. \quad (25)$$

Now, specify the asymptotic expansions in the form

$$f = f^{(0)} + \eta f^{(1)} + \dots \quad (26)$$

where  $f = (u^*, \sigma_{31}^*, \sigma_{32}^*)$ .

At leading order, we have from (23)

$$\sigma_{32}^{(0)} = u_{,\zeta}^{(0)}. \quad (27)$$

Then, we substitute this formula in Eq. (21). Next, integrating in the transverse variable  $\zeta$  and satisfying the boundary condition (24) along the clamped lower face of the coating, we obtain

$$u^{(0)} = B_0 \sin \Omega \zeta, \quad (28)$$

where  $B_0(\xi)$  denotes the unknown 1D displacement amplitude. Here and below, the time-harmonic factor is omitted. The remaining stress takes the form

$$\sigma_{31}^{(0)} = B_{0,\xi} \sin \Omega \zeta. \quad (29)$$

Thus, as usual, the leading order approximation does not result in a differential equation for the sought for vibration amplitude. Moreover, the substitution of (29) in the boundary condition (25) gives zero at the cut-off frequencies  $\Omega = \Omega_*$  (see (14)). As a result, we have to proceed to the next order approximation.

At next order, Eq. (23) reduces to

$$\sigma_{32}^{(1)} = u_{,\zeta}^{(1)} - i\Omega u_{,\zeta}^{(0)}. \quad (30)$$

Then, we insert the latter into (21) and integrate in  $\zeta$ , having an inhomogeneous equation given by

$$u_{,\zeta\zeta}^{(1)} + \Omega^2 u^{(1)} = -(B_{0,\xi\xi} + i\Omega^3 B_0) \sin \Omega \zeta. \quad (31)$$

Its solution, satisfying the boundary condition (24), is

$$u^{(1)} = B_1 \sin \Omega \zeta + (B_{0,\xi\xi} + i\Omega^3 B_0) \frac{\zeta \cos \Omega \zeta}{2\Omega}. \quad (32)$$

The imaginary term in this formula corresponds to the effect of viscosity which does not appear at leading order.

Now, using (28) and (32), we may present the two-term expansion ( $u^* = u^{(0)} + \eta u^{(1)} + \dots$ ) as

$$u^* = B \sin \Omega \zeta + \eta (B_{,\xi\xi} + i\Omega^3 B) \frac{\zeta \cos \Omega \zeta}{2\Omega} + O(\eta^2), \quad (33)$$

where  $B = B_0 + \eta B_1$ .

Finally, substituting the derived expansion in the boundary condition (25) at the upper face, we arrive at the 1D equation of interest. It is given by

$$\eta T \frac{d^2 B}{d\xi^2} + QB = 2\Omega P^*. \quad (34)$$

where

$$T = \cos \Omega - \Omega \sin \Omega, \quad Q = Q_1 - iQ_2 \quad (35)$$

with

$$Q_1 = 2\Omega^2 \cos \Omega, \quad Q_2 = \eta \Omega^3 (\cos \Omega + \Omega \sin \Omega) \quad (36)$$

#### 4. Discussion and numerical visualization

Let us rewrite the Eq. (34) for the displacement at the upper face ( $\zeta = 1$ ). In a dimensional form, it becomes

$$H^2 T \frac{d^2 w}{dx_1^2} + Qw = \frac{2PH}{\mu} \Omega \sin \Omega, \quad (37)$$

where  $w = BH \sin \Omega$  (see (33)). This equation has the form similar to those for high-frequency, long-wave vibration governing a single mode in the vicinity of thickness resonance frequencies (e.g. see [10, 11, 15–17, 20]). However, in contrast to the latter equation, (37) is of multimode nature governing long-wave behaviour near each of the cut-offs. This results in a sophisticated dependence of the coefficients  $T$  and  $Q$  given by (35), (36) on the frequency parameter  $\Omega$ . To have a further insight, look at the associated dispersion relation

$$TK^2 - Q = 0. \quad (38)$$

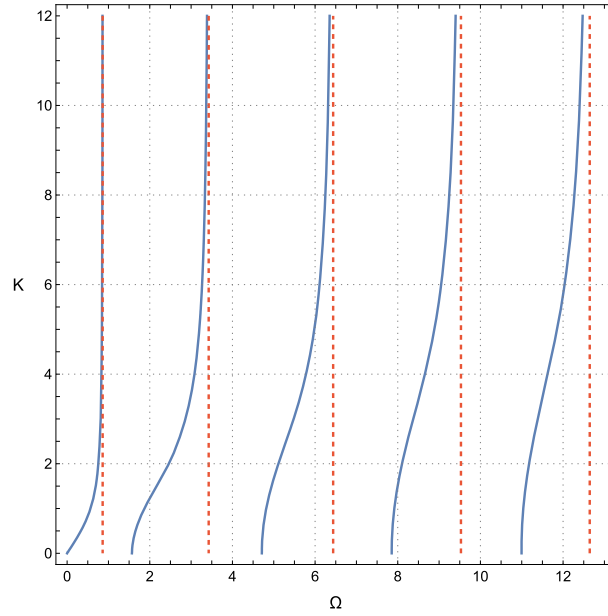


FIG. 2. Dispersion curves (blue solid) for an elastic coating calculated from the asymptotic relation (38). The vertical dashed lines correspond to  $T = 0$  (Eq. (35)) (Color figure online)

The dispersion curves for purely elastic set-up ( $\eta = 0$ ) are displayed in Fig. 2. It is remarkable that the multimode formulation predicts a spurious fundamental (low-frequency) mode which is not the feature of the original antiplane problem (see Sect. 2). It is interesting that analysis of the denominator in formula (15) corresponding to the exact solution of the time-harmonic problem for forced vibrations may hypothetically assume that the dispersion relation takes the form

$$\alpha \cos \alpha = 0 \quad (39)$$

instead of the correct one determined by (12). It can easily be verified that the asymptotic behaviour of (39) is given by the shortened dispersion relation (38) with both of them supporting a spurious fundamental mode. The latter observation complements the discussion initiated in Sect. 2.

The short-wave limit of the dispersion curves in Fig. 2 corresponds to the vertical asymptotes given by  $T = 0$  for which Eq. (37) degenerates. However, it happens outside the validity range of the developed model oriented to long-wave motions near the cut-offs  $\Omega = \Omega_*$  (see (14)). In this case, the dispersion relation (38) can be reduced to

$$K^2 \approx \Omega_*^2(\Omega^2 - \Omega_*^2 + i\eta\Omega_*), \quad (40)$$

which also determines a near cut-off asymptotic behaviour of the original dispersion relation (12) at  $\eta \ll 1$ . The numerical data are presented in Fig. 3 for the real and imaginary parts of the squared wavenumber at  $\eta = 0.01$ .

The results for the dispersion relations (12) and (38) are compared. As might be expected, the asymptotics in Fig. 3 for the real parts are applicable near the cut-offs. This observation is also true for the imaginary parts (see Fig. 4), but, to the best of our knowledge, such comparison has not been demonstrated before.

Next, discuss the inhomogeneous Eq. (37) in application to modelling of long-wave forced vibrations over a broad frequency range, including several propagating modes. In this case, the Fourier transform

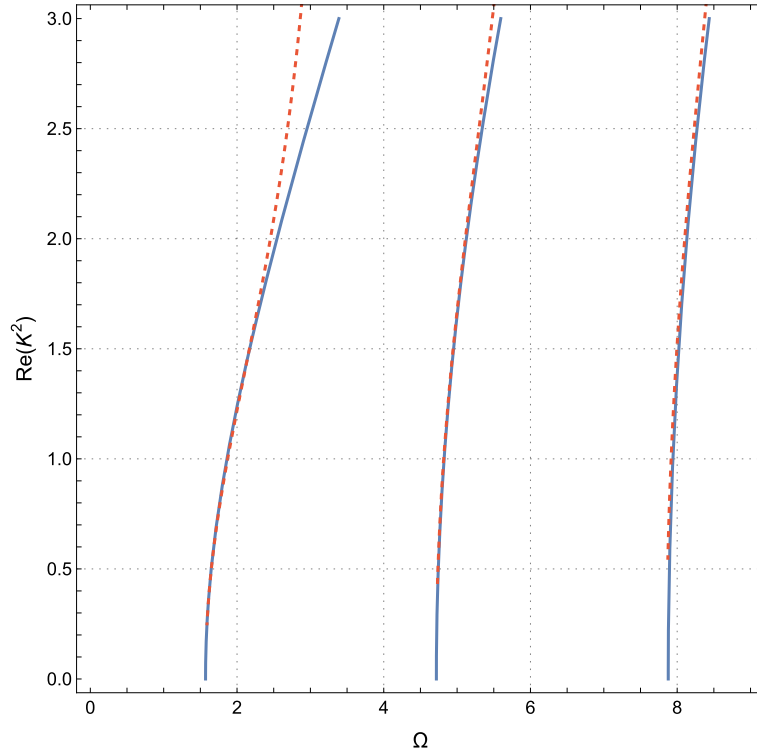


FIG. 3. The real part of  $K^2$  for exact (Eq. (12), solid blue lines) and asymptotic (Eq. (38), red dashed lines) dispersion relations at  $\eta = 0.01$  (Color figure online)

of the solution to the aforementioned equation, rewritten in the dimensionless variable  $\xi$ , becomes

$$w^F = -\frac{2P^F}{TK^2 - Q} \sin \Omega, \quad (41)$$

where we adapt the same definition of the Fourier transform as in Sect. 2.

It can readily be verified by applying Taylor series expansions at  $K \ll 1$  that the asymptotic behaviour of the exact Fourier transform of  $u^F$  given by (15) at  $\zeta = 1$  is identical to (41). This observation motivates comparison of the inverse Fourier transforms corresponding to (41) and (15) aiming at estimating the accuracy of the former for dynamic loadings involving not only long-wave ( $K \ll 1$ ) but also short-wave components ( $K \gtrsim 1$ ) for which the developed asymptotic model is generally not valid.

As an example, we consider the effect of  $\delta$ -like time-harmonic concentrated load for which

$$P = P_0 \delta_\varepsilon(\xi) \quad (42)$$

in which

$$\delta_\varepsilon^F = \frac{1}{1 + \varepsilon K^2} \quad (43)$$

where the upper suffix  $F$  denotes the Fourier transform as above, and  $\varepsilon$  is a relatively small quantity.

Below we compare numerically the following inverse Fourier transforms

$$u = \frac{1}{\pi} \int_0^\infty u^F \cos(K\xi) dK, \quad w = \frac{1}{\pi} \int_0^\infty w^F \cos(K\xi) dK, \quad (44)$$

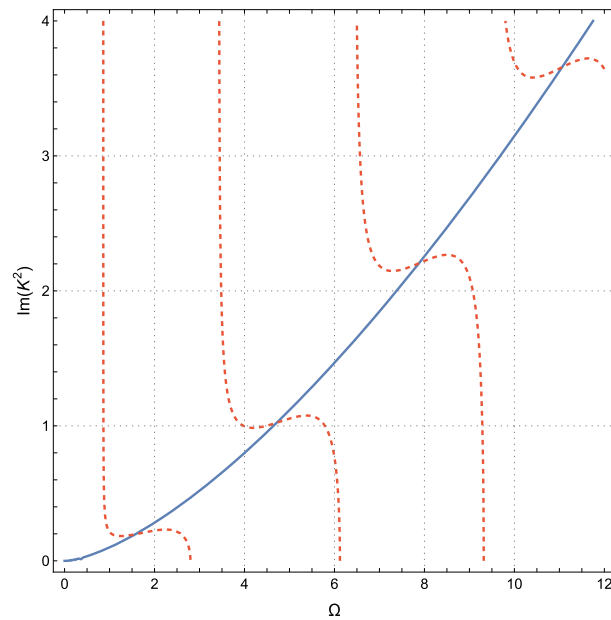


FIG. 4. The imaginary part of  $K^2$  for exact (Eq. (12), solid blue lines) and asymptotic (Eq. (38), red dashed lines) dispersion relations at  $\eta = 0.01$  (Color figure online)

where  $u^F$  and  $w^F$  are given by the expressions (15) and (41) at  $\zeta = 1$ , respectively, taking into account (43). In Fig. 5, we plot the functions

$$(\bar{u}, \bar{w}) = \frac{\mu}{P_0 H} |(u, v)| \quad (45)$$

versus the dimensionless frequency  $\Omega$  at  $\varepsilon = 0.01$  and  $\eta = 0.005$ . It is clearly seen that the jumps of the function  $\bar{u}$  near the cut-offs  $\Omega = \Omega_*$  is reasonably well approximated by those of the function  $\bar{w}$ . In this case, both of the functions have a double pole at the origin  $K = 0$  perturbed by a small imaginary term with the factor  $i\eta$ . As a result, the contribution of the related residues is  $\sim 1/\sqrt{\eta}$ . Similar spikes are typical for the time-harmonic vibrations of an elastic layer subject to a light fluid loading (see [11, 20]). For the latter, elastic vibrations are damped due to the acoustic radiation into the fluid. Figure 7 plotted at the same value of  $\eta$  clearly demonstrates that the asymptotic model is highly accurate over the long-wave domain,  $K \ll 1$ , at the first thickness resonance frequency  $\Omega_* = \pi/2$ .

At the same time, Eq. (37) does not pretend to describe the short-wave behaviour corresponding to small amplitude plateaus of  $O(1)$  outside the observed sharp peaks. In addition, the derived 1D Eq. (37) predicts spurious peaks in Fig. 5 at  $T = 0$  (e.g. for  $\Omega \approx 0.86$ ) where, as it has already been mentioned, it degenerates. This effects the convergence of the second integral in (44) (see Fig. 6), illustrating a drastical discrepancy of the Fourier transforms (15) and (41) at  $\Omega = 0.86$  for  $\eta = 0.01$ .

## 5. Concluding remarks

The derived 1D Eq. (37) governs long-wave behaviour of all vibration modes (14). The price of such generality is that the coefficients in this equation depend on the frequency parameter  $\Omega$  (see (35) and (36)). The time-harmonic set-up underlying (37) may be potentially extended to arbitrary time dependence by the formal substitution  $\Omega = (-i d/dt)\sqrt{\rho/\mu}H$ . In this case, however, due to the presence of trigonometric



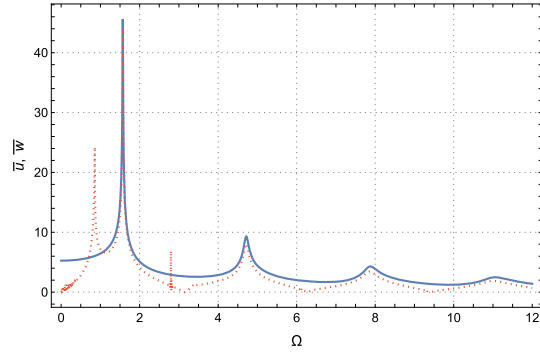


FIG. 5. Comparison of the exact (solid blue line) and asymptotic (red dashed line) formulae in (45) for displacements at  $\varepsilon = 0.01$  and  $\eta = 0.005$  (Color figure online)

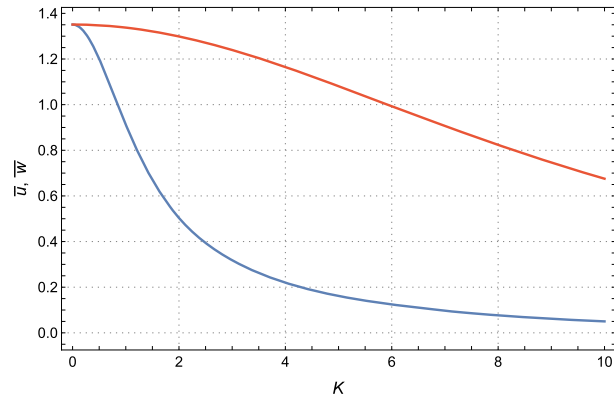


FIG. 6. Comparison of the exact (blue line) and asymptotic (red line) Fourier transforms (see, (15) and (41)) at the first spurious spike  $\Omega = 0.86$  at  $\varepsilon = 0.01$  and  $\eta = 0.01$  (Color figure online)

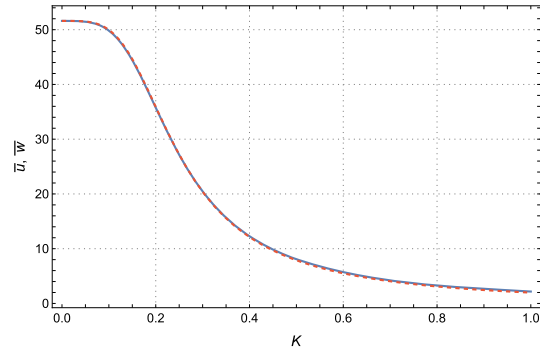


FIG. 7. Comparison of the exact (blue line) and asymptotic (red line) Fourier transforms (see, (15) and (41)) at the first thickness resonance frequency  $\Omega = \Omega_* = \pi/2$ ,  $\varepsilon = 0.01$  and  $\eta = 0.01$  (Color figure online)

functions in the coefficients (35) and (36), the amended equation will have coefficients expressed through pseudo-differential operators of time.

The associated dispersion relation (38) also seems to be a novel outcome. It nicely approximates the dispersion curves near the cut-off frequencies  $\Omega_*$  given by (14), as illustrated by comparison with the exact solution (13) (see Figs. 3 and 4). At the same time, this dispersion relation supports an additional low-frequency mode (see Fig. 2), which obviously does not exist in the original 2D model of a coating. This figure also demonstrates vertical asymptotes corresponding to the prohibited (within the developed long-wave model) short-wave limit at  $T = 0$ , where  $T$  is the coefficient of the senior derivative in equation (37).

At the frequencies corresponding to the aforementioned asymptotes, the spurious peaks occur (see Fig. 5). This figure is aimed at testing the asymptotic predictions for the problem considering the effect of a  $\delta$ -type concentrated load. It is more important, however, that all the peaks at the cut-offs in Fig. 5 are accurately approximated (see also comparison in Fig. 7). The amplitude of these peaks is  $\sim 1/\eta$  exceeding considerably the background level formed by short-wave patterns. Similar peaks arise in the problem for a fluid-loaded elastic layer subject to a time-harmonic point force (see [20]). We also note that multimode long-wave approximations are universally valid for smoothly distributed loads that do not induce short wavelength vibrations (see [23]).

The proposed asymptotic methodology is apparently not restricted to the considered scalar problem. The general idea of multimode long-wave approximations may be adapted for more elaborated scenarios, including but not restricted to a similar problem for a 3D coating. The simplest Voight model implemented in the paper may also be extended to more advanced formulations for viscoelastic behaviour, since only a relatively small viscous damping near the cut-offs is essential.

**Author contributions** All authors contributed equally to the manuscript.

**Funding** BE acknowledges the support of The Scientific and Technological Research Council of Türkiye (Tübitak) under the Grant No.: 222N095. Authors MI, JK and DP acknowledge the German Research Foundation (DFG) for supporting this research under the Grant No.: 520432297.

**Data availability** No data sets were generated or analysed during the current study.

**Declarations**

**Conflict of interest** The authors declare that they have no conflict of interest.

**Ethics approval and consent to participate** Not Applicable.

**Open Access.** This article is licensed under a Creative Commons Attribution 4.0 International License, which permits use, sharing, adaptation, distribution and reproduction in any medium or format, as long as you give appropriate credit to the original author(s) and the source, provide a link to the Creative Commons licence, and indicate if changes were made. The images or other third party material in this article are included in the article's Creative Commons licence, unless indicated otherwise in a credit line to the material. If material is not included in the article's Creative Commons licence and your intended use is not permitted by statutory regulation or exceeds the permitted use, you will need to obtain permission directly from the copyright holder. To view a copy of this licence, visit <http://creativecommons.org/licenses/by/4.0/>.

**Publisher's Note** Springer Nature remains neutral with regard to jurisdictional claims in published maps and institutional affiliations.

## References

- [1] Goldenveiser, A.L.: The general theory of elastic bodies (shells, coatings and linings). *Mech. Sol.* **3**(3), 17 (1992)

- [2] Lenser, A Aghalovyan: Asymptotic Theory of Anisotropic Plates and Shells. World Scientific, Singapore (2015)
- [3] Hauert, R.: A review of modified DLC coatings for biological applications. *Diamond Related Mater.* **12**(3–7), 583–589 (2003)
- [4] Pawlowski, L.: The Science and Engineering of Thermal Spray Coatings. Wiley, New York (2008)
- [5] Li, M., Liu, Q., Jia, Z., Xu, X., Cheng, Y., Zheng, Y., Xi, T., Wei, S.: Graphene oxide/hydroxyapatite composite coatings fabricated by electrophoretic nanotechnology for biological applications. *Carbon* **67**, 185–197 (2014)
- [6] Bose, S.: High Temperature Coatings. Butterworth-Heinemann (2017)
- [7] Sathish, M., Radhika, N., Saleh, Bassiouny: A critical review on functionally graded coatings: methods, properties, and challenges. *Compos. Part B Eng.* **225**, 109278 (2021)
- [8] Alshits, V.I., Maugin, G.A.: Dynamics of multilayers: elastic waves in an anisotropic graded or stratified plate. *Wave Motion* **41**(4), 357–394 (2005)
- [9] Lutanov, M., Rogerson, G.A.: The influence of boundary conditions on dispersion in an elastic plate. *Mech. Res. Commun.* **37**(2), 219–224 (2010)
- [10] Lashhab, M.I., Rogerson, G.A., Prikazchikova, L.A.: Small amplitude waves in a pre-stressed compressible elastic layer with one fixed and one free face. *Z. Angew. Math. Phys.* **66**, 2741–2757 (2015)
- [11] Kaplunov, J.D., Yu Kossovich, L., Nolde, E.V.: Dynamics of Thin Walled Elastic Bodies. Academic Press, Cambridge (1998)
- [12] Kaplunov, J.D.: Long-wave vibrations of a thinwalled body with fixed faces. *Q. J. Mech. Appl. Math.* **48**(3), 311–327 (1995)
- [13] Berdichevskii, V.L.: High-frequency long-wave vibrations of plates. In: *Soviet Physics Doklady*, Vol. 22, p. 604 (1977)
- [14] Le, K.C.: High frequency vibrations and wave propagation in elastic shells: variational-asymptotic approach. *Int. J. Solids Struct.* **34**(30), 3923–3939 (1997)
- [15] Rogerson, G.A., Prikazchikova, L.A.: Generalisations of long wave theories for pre-stressed compressible elastic plates. *Int. J. Nonlinear Mech.* **44**(5), 520–529 (2009)
- [16] Pichugin, A.V., Rogerson, G.A.: A two-dimensional model for extensional motion of a pre-stressed incompressible elastic layer near cut-off frequencies. *IMA J. Appl. Math.* **66**(4), 357–385 (2001)
- [17] Pichugin, A.V., Rogerson, G.A.: Anti-symmetric motion of a pre-stressed incompressible elastic layer near shear resonance. *J. Eng. Math.* **42**, 181–202 (2002)
- [18] Erbaş, B., Kaplunov, J., Nolde, E., Palsü, M.: Composite wave models for elastic plates. *P. Roy. Soc. A-Math. Phys.* **474**(2214), 20180103 (2018)
- [19] Erbaş, B., Kaplunov, J., Palsü, M.: A composite hyperbolic equation for plate extension. *Mech. Res. Commun.* **99**, 64–67 (2019)
- [20] Kaplunov, J.D., Markushevich, D.G.: Plane vibrations and radiation of an elastic layer lying on a liquid half-space. *Wave Motion* **17**(3), 199–211 (1993)
- [21] Goldenveizer, A.L.: Theory of Elastic Thin Shells: Solid and Structural Mechanics, Vol. 2. Elsevier, Great Britain, (2014)
- [22] Goldenveizer, A.L., Lidsky, V.B., Tovstik, P.E.: Free Vibrations of Thin Shells. Nauka, Moscow (1978). ((in Russian))
- [23] Cherednichenko, K., Kaplunov, J., Prikazchikov, D., Sultanova, L.: Global long wave approximations for elastic wave guides. In: 11th International Conference on Structural Dynamic, EUROLYN, pp. 2464–2474. ICMES (2020)

Barış Erbaş  
 Department of Mathematics  
 Eskisehir Technical University  
 Yunus Emre Campus  
 26470 Eskisehir  
 Turkey  
 e-mail: [berbas@eskisehir.edu.tr](mailto:berbas@eskisehir.edu.tr)

Mikhail Itskov and Julius Kaplunov  
 Department of Continuum Mechanics  
 RWTH Aachen University  
 52062 Aachen  
 Germany  
 e-mail: [itskov@km.rwth-aachen.de](mailto:itskov@km.rwth-aachen.de)

Julius Kaplunov  
 e-mail: [j.kaplunov@keele.ac.uk](mailto:j.kaplunov@keele.ac.uk)

Mikhail Itskov, Julius Kaplunov and Danila Prikazchikov  
School of Computer Science and Mathematics  
Keele University  
Keele ST5 5BG  
UK  
e-mail: d.prikazchikov@keele.ac.uk

(Received: October 27, 2024; revised: October 28, 2024; accepted: November 4, 2024)